N-Site approximations and CAM analysis for a stochastic sandpile

Ronald Dickman†
Departamento de Fí sica, ICEx, Universidade Federal de Minas Gerais, Caixa Postal 702, 30161-970 Belo Horizonte, MG, Brazil
(February 1, 2008)

Abstract

I develop n-site cluster approximations for a stochastic sandpile in one dimension. A height restriction is imposed to limit the number of states: each site can harbor at most two particles (height $z_i \leq 2$). (This yields a considerable simplification over the unrestricted case, in which the number of states per site is unbounded.) On the basis of results for $n \leq 11$ sites, I estimate the critical particle density as $\zeta_c = 0.930(1)$, in good agreement with simulations. A coherent anomaly analysis yields estimates for the order parameter exponent [$\beta = 0.41(1)$] and the relaxation time exponent ($\nu_{||} \simeq 2.5$).

I. INTRODUCTION

Sandpile models are the prime example of self-organized criticality (SOC) [1,2], in which a system with an absorbing-state phase transition is forced to its critical point [3–5], leading to scale-invariance in the apparent absence of parameters [6]. The absorbing-state phase transition, which depends, as is usual, on the fine-tuning of one or more control parameters, is evident in sandpiles with a fixed number of particles [3,7–10], models that have come to be called fixed-energy sandpiles (FES). While most studies of sandpiles have probed the driven case [2,14], there is great interest in understanding the scaling properties of FES models as well [9,11–13].

Previous studies of FES reveal that they exhibit a phase transition between an absorbing and an active state as the particle density ζ (which is the temperaturelike control parameter) is increased beyond a critical value [3,15,16]. Until now, all quantitative results on FES have been obtained from simulations. It is therefore of interest to apply theoretical methods to such models. One such approach is Suzuki's coherent anomaly method (CAM) for analyzing a series of cluster approximations. It has been shown to yield good estimates for critical properties both in [17,18] and out of equilibrium [19,20]. In this work I develop n-site approximations for a one-dimensional sandpile model, and analyze the results using the CAM. This represents the first application of the CAM to a model representative of the class of absorbing-state phase transitions in systems with a conserved density [21–23].

In this paper I study a FES with a height restriction. From the theoretical viewpoint, an inconvenient feature of sandpile models is the unbounded number of particles that may occupy the same site; this complicates attempts to derive cluster approximations. In Manna's stochastic sandpile [24,25], sites with height $z \geq 2$ are active. If we restrict the height (or number of sand grains per site), to be ≤ 2, the effect on critical properties should be minimal, aside from a possible shift in the critical density ζ_c. This expectation was recently verified numerically: the restricted-height stochastic sandpile belongs to the same universality class as its unrestricted counterpart [26]. I study the restricted-height model for calculational convenience, as a representative of a broader universality class that includes Manna's stochastic sandpile, the conserved lattice gas, and the conserved threshold transfer process [21].

The balance of the paper is organized as follows. The model is defined in Sec. II, followed by a discussion of n-site approximations in Sec. III. Numerical results are presented in Sec. IV. The CAM analysis is discussed in Sec. V, and in Sec. VI I present a brief summary.

II. MODEL

The model is defined on a ring of L sites with periodic boundaries. (The cluster approximations effectively study the $L \to \infty$ limit.) The configuration is specified by the number of particles $z_i = 0, 1$, or 2 at each site; sites with $z_i = 2$ are said to be *active*, and have a toppling rate of unity. The continuous-time (sequential), Markovian dynamics consists of a series of toppling events at individual sites. When site i topples, two particles attempt move to randomly chosen nearest neighbors j and j' of i. The new position of each particle is accepted if and only if the target site has fewer than two particles. I consider a stochastic toppling rule in which the two particles move independently. Any particle attempting to move to a site already harboring two particles is sent back to the toppling site. (Thus an

attempt to send two particles from site j to site k, with $z_k = 1$, results in $z_k = 2$ and $z_j = 1$.) Transition probabilities are listed in Table I.

This model, and a closely related one (with a cooperative toppling rule), were studied via simulation in Ref. [26], which showed that the critical exponents β and $\nu_\perp$ are the same as for the unrestricted Manna sandpile. A similar conclusion was reached in Ref. [21] for a two-dimensional restricted-height sandpile (called the conserved threshold transfer process in that work).

III. CLUSTER APPROXIMATIONS

I have derived dynamic n-site cluster approximations for the one-dimensional restricted sandpile model. Such approximations often yield qualitatively correct phase diagrams [27]. The procedure parallels that used by Ferreira and Mendirata to study the one-dimensional contact process [20]. The n-site approximation consists of a set of coupled differential equations for the probabilities $P_{\mathcal{C}}^{(n)}$ of each n-site configuration, $\mathcal{C}$. (There are 3^n such configurations, but the number of independent probabilities is $\sim 3^n/2$, due to symmetries.) The system is assumed homogeneous, so that the $P_{\mathcal{C}}^{(n)}$ are independent of position.

Since transitions in a set of n contiguous sites generally depend on sites outside the cluster, the n-site probabilities are coupled to those for $n{+}1$ and so on, generating an infinite hierarchy of equations. The n-site approximation truncates this hierarchy by approximating m-site probabilities (for $m > n$) in terms of n-site *conditional* probabilitites. In the n-site approximation, the joint probability for a sequence of $n{+}1$ sites is approximated so [20]:

$$\begin{aligned} P^{(n+1)}(z_1, ..., z_{n+1}) &\simeq P^{(n)}(z_{n+1}|z_n, ..., z_2) P^{(n)}(z_n, ..., z_1) \\ &= \frac{P^{(n)}(z_{n+1}, ..., z_2) P^{(n)}(z_n, ..., z_1)}{P^{(n-1)}(z_n, ..., z_2)} \ . \end{aligned} \tag{1}$$

The equations for one- and two-site approximations are relatively simple to derive, and are described in Ref. [26]. I have developed a computational algorithm capable of generating the approximation for arbitrary n. Each configuration $\mathcal{C} = (z_n, ..., z_1)$ is represented by an integer

$$I(\mathcal{C}) = \sum_{k=1}^{n} z_k \cdot 3^{k-1} \ . \tag{2}$$

The calculation begins with the generation of all configurations, corresponding to each integer from zero (all sites empty) up to the maximum, $3^n - 1$ (all sites doubly occupied); the symmetry (under inversion) of each configuration is determined. If $\mathcal{C}$ is not symmetric, then it and its mirror image $\mathcal{C}_R$ must have the same probability, and only the smaller of $\mathcal{C}$ and $\mathcal{C}_R$ is treated explicitly, reducing the number of variables by roughly half.

Next, a list of all possible transitions is constructed. Here it is useful to distinguish between *central* transitions (involving a toppling at one of the sites 2,...,$n{-}1$) and *boundary* transitions, in which either site 1 or site n, or one of the peripheral sites (0 or $n{+}1$) topples. The rate of a central transition $\mathcal{C} \to \mathcal{C}'$ is the product of a branching probability p_b (for the particles to be redistributed in a particular manner, as in Table I), and the intrinsic toppling

rate, which is unity. Consider, for example, configuration $\mathcal{C} = (21120)$. The transition rates associated with a toppling at the second site (counting from the right), are

$$w[(21120) \to (21102)] = \frac{1}{4},$$

$$w[(21120) \to (21201)] = \frac{1}{2},$$

$$w[(21120) \to (21210)] = \frac{1}{4}.$$

For each configuration $\mathcal{C}$, the set of allowed transitions to other states, and the associated rates, are stored. In the case of a central transition from $\mathcal{C}$ to $\mathcal{C}'$, the contribution to the time-derivative of the probability has the form:

$$\frac{dP(\mathcal{C}')}{dt} = w[\mathcal{C} \to \mathcal{C}']P(\mathcal{C}).$$

There is of course a corresponding loss term for $P(\mathcal{C})$:

$$\frac{dP(\mathcal{C})}{dt} = -w[\mathcal{C} \to \mathcal{C}']P(\mathcal{C}).$$

Thus central transitions contribute to the evolution of the probability distribution precisely as in the master equation.

For boundary transitions, one does not have access to the $n+1$-site probabilitites required to mount a complete description, and so must resort to the truncation scheme embodied in Eq. (1). For example, the contribution to $dP(2, z_2, ..., z_n)/dt$ due to the transition $(2, z_2, ..., z_n) \to (1, z_2, ..., z_n)$ is

$$\frac{1}{2}P^{(n+1)}(0, 2, z_2, ..., z_n) + \frac{3}{4}P^{(n+1)}(1, 2, z_2, ..., z_n) \ .$$

The $P^{(n+1)}$ are estimated using Eq. (1). For boundary transitions one stores not only the rate, but the two configurations (aside from the original one, $\mathcal{C}$) whose probabilities are needed to evaluate $dP(\mathcal{C})/dt$. With this information available, one can evaluate the derivatives $dP(\mathcal{C})/dt$ for all possible configurations, given the probability distribution.

The evolution of the probability distribution is found via numerical integration, using a fourth-order Runge-Kutta scheme [28]. The integration is halted when a stationary distribution is attained, that is, when the time-derivatives $dP(\mathcal{C})/dt$ all have an absolute value smaller than δ (typically, $\delta = 10^{-13}$). An interesting technical point concerns the evaluation of the $n-1$-site marginal distribution. There are evidently two equivalent expressions that may be used:

$$P^{(n-1)}(z_{n-1}, ..., z_1) = \sum_{z_n=0}^{2} P^{(n)}(z_n, z_{n-1}, ..., z_1) \ ,$$

and

$$P^{(n-1)}(z_{n-1},...,z_1) = \sum_{z_0=0}^{2} P^{(n)}(z_{n-1},...,z_1,z_0) \ .$$

Numerical stability is *greatly enhanced* using the *mean* of the two expressions given above.

For sizes $n \geq 7$, very near the critical point, relaxation to the stationary distribution is very slow, and the following procedure proves advantageous. Let $D = \max_{\mathcal{C}} |dP(\mathcal{C})/dt|$ be the largest derivative (in absolute value). The properties of interest (principally, the active-site density) are recorded as a function of D, and the integration halted when $D < 10^{-10}$. Fig. 1 shows the result for the active site density, for ζ slightly above ζ_c. The stationary value is obtained via extrapolation to $D = 0$, usually via a quadratic fit to the four data points for smallest D. (The resulting correction is typically less than 1% of the value at $D = 10^{-10}$.) I also studied the order parameter relaxation rate $\gamma = |\dot{\rho}/\rho|$ for each n at a series of ζ values near, but below, ζ_c. These data are used to estimate the critical exponent $\nu_{||}$ in Sec. V.

IV. NUMERICAL RESULTS

I derived cluster approximations for $n \leq 11$ sites, yielding the stationary active-site density ρ_a as a function of ζ. The n-site approximation predictions for $\rho_a(\zeta)$ ($n = 3$ to 11) are compared against simulation in Fig. 2; the theoretical curves appear to approach the simulation result systematically.

For each n, the active-site density is zero below a certain critical value, $\zeta_{c,n}$. Since the phase transition in the stochastic sandpile is continuous [16,26], one expects the same to be true of the cluster approximations. This is indeed the case for $n \leq 4$, but for $n = 5$, 6 and 7 there is a very small discontinuity in ρ_a ($\lesssim 10^{-3}$, invisible on the scale of Fig. 2), as we decrease ζ. Since the same procedure is used for all n, the discontinuity is unlikely to be artefact of the numerical method. On the other hand, I do not regard the discontinuity as physically significant; it appears to represent an unphysical feature of the cluster approximations for certain n values, very near the critical density. In the CAM analysis I disregard the behavior of ρ_a in the immediate vicinity of $\zeta_{c,n}$, and instead analyze its properties at points somewhat removed from the transition.

There remains, naturally, the problem of estimating the critical density, $\zeta_{c,n}$. For each n I determine the critical density by fitting the four or five data points nearest the transition, where $\rho \simeq 10^{-3}$ or less. In each case, I plot $\ln \rho_a$ versus $\ln(\zeta - \zeta_{c,n})$, varying $\zeta_{c,n}$ to obtain the best power-law fit. The associated slopes vary between 1 (for $n = 3$) and about 0.25 (for $n = 6$), but these, again, are regarded as unimportant details of the approximation in question. It is important to stress that, in the cases where the transition is apparently discontinuous, the difference between the location of the discontinuity and the extrapolated value of $\zeta_{c,n}$ is less than one part in 10^5, and that the estimates for ζ_c and critical exponents are insensitive to these tiny differences. The values of $\zeta_{c,n}$ obtained in this manner are listed in Table II.

Using the results for $\zeta_{c,n}$, I estimate $\zeta_c = \lim_{n\to\infty} \zeta_{c,n}$ by plotting $\Delta_n \equiv \zeta_c - \zeta_{c,n}$ versus n in a double-logarithmic plot, varying ζ_c to obtain the best power-law fit. The latter is obtained using ζ_c in the range 0.929 - 0.931, yielding $\zeta_c = 0.930(1)$, in good agreement with the simulation result of 0.92965 [26]. The finite-size scaling prediction for the critical point

shift is [29]: $\Delta_n^{\nu_\perp} \propto 1/n$. I obtain a good fit to the data (see Fig. 3) using $\nu_\perp = 1.66$ (as found in simulations [16,26]), including a correction to scaling term:

$$\Delta_n^{\nu_\perp} \propto \frac{A}{n} + \frac{B}{n^2} \ .$$

The numerical data are consistent with the simulation estimate for $\nu_\perp$, but not sufficient to furnish an independent estimate of the exponent.

V. COHERENT ANOMALY ANALYSIS

A detailed explanation of the CAM procedure is given in Ref. [17,18]; it may be understood on the basis of finite-size scaling [29]. The approach here parallels that used by Tomé and de Oliveira in their study of the Domany-Kinzel model [30]. To begin, one argues that the cluster size n plays the role of an effective system size L as regards scaling properties. This is because the n-site approximation effectively cuts off correlations of range $> n$ (notwithstanding the fact that cluster approximations nominally treat an infinite system). Thus, as noted above, one expects a critical point shift $\Delta_n \propto n^{-1/\nu_\perp}$. Finite-size scaling theory also yields the relation $\rho_{a,n}(\zeta_c) \propto n^{-\beta/\nu_\perp} \propto \Delta_n^\beta$ for the order parameter in a finite system, at the (true) critical point. For $\zeta > \zeta_{c,n}$, $\rho_{a,n}(\zeta)$ is a smooth function. Thus we are led to a scaling hypothesis for the order parameter [30]:

$$\rho_{a,n}(\zeta) = \Delta_n^\beta f\left(\frac{\zeta - \zeta_{c,n}}{\Delta_n}\right), \tag{3}$$

where $f(x)$ is a scaling function with $f(0)=0$. If we suppose that $f(x) \propto x^{\beta_{MF}}$ for $0 \le x \le 1$, then $\rho_{a,n}(\zeta) = A_n(\zeta - \zeta_{c,n})^{\beta_{MF}}$, where the amplitude A_n diverges as $n \to \infty$:

$$A_n \propto \Delta_n^{-(\beta_{MF}-\beta)}. \tag{4}$$

This is the usual CAM relation. On the other hand, the hypothesis that n is equivalent to a finite system size leads directly to:

$$\rho_{a,n}(\zeta_c) \sim \Delta_n^\beta. \tag{5}$$

This expression involves the behavior of the n-site approximation at the critical point ζ_c not $\zeta_{c,n}$. It is interesting to note that the hypothesis of an effective system size directly proportional to n is not strictly necessary. The scaling relations involving Δ_n follow from the more general hypothesis of an effective system size $L_{eff} = L_{eff}(n)$, for example $L_{eff} \propto n^\phi$ with $\phi > 0$.

A. CAM analysis for β

As noted above, the n-site approximations for the order parameter $\rho_{a,n}$ are not all well behaved in the vicinity of $\zeta_{c,n}$. For this reason, analysis of $\rho_{a,n}$ at $\zeta_{c,n}$ will not yield a consistent set of well defined amplitudes A_n. But since $\rho_{a,n}(\zeta)$ is well behaved for $\zeta > \zeta_{c,n}$,

we can study its scaling at some point intermediate between $\zeta_{c,n}$ and ζ_c. In particular, the scaling hypothesis Eq. (3) implies that if we fix $x = (\zeta - \zeta_{c,n})/\Delta_n$, then

$$\frac{d\rho_{a,n}}{d\zeta} = f(x)\Delta_n^{\beta-\beta_{MF}}. \tag{6}$$

Our strategy is to analyze the order parameter data reasonably near the n-site critical value, but away for $\zeta_{c,n}$ itself, where $\rho_{a,n}$ is singular. A crucial point in this analysis is the postulate that the mean-field exponent $\beta_{MF} = 1$, *regardless of the behavior of* $\rho_{a,n}$ *in the immediate vicinity of* $\zeta_{c,n}$. The motivation for this assumption is, firstly, that β_{MF} is clearly unity for $n = 1$, 2, or 3; secondly, that a critical exponent such as β is determined, in mean-field theory, by symmetry properties of the order parameter, and hence should not vary with n; and thirdly, that $\beta_{MF} = 1$ generically for phase transitions to an absorbing state [27]. (The basis for this last assertion is that the mean-field equation for the order parameter will have the form $d\rho/dt = A\rho - B\rho^2$, barring some coincidence or a symmetry that renders A and/or B zero [31].)

I evaluate $d\rho_{a,n}/d\zeta$ (numerically, using an interval $\Delta = 0.0005$), for fixed $x = 1/4$; the results are shown in Fig. 4. Least-squares linear fits to the data for $n = 8$ - 11 yield, via Eq. (6), the value $\beta = 0.408(6)$, where the figure in parenthesis denotes the uncertainty. Using $\zeta_c = 0.929$ instead of the best estimate, 0.930, I find $\beta = 0.421(5)$. Thus a reasonable estimate for β is 0.41(1). (A similar analysis, but evaluating the derivatives at $x = 1/2$, yields $\beta = 0.42$.)

The above analysis is complemented with a study of $\rho_{a,n}(\zeta_c)$, as suggested by Eq. (5). The graph of $\rho_{a,n}(\zeta_c)$ versus Δ_n shows (on log scales, see Fig. 5), a fair amount of curvature, making determination of β more difficult in this case. Linear fits to the data for n = 7-9, 8-10, and 9-11 yield, respectively, $\beta = 0.471$, 0.460, and 0.448, consistent with an approach to the value of 0.41 for large n. Verification of convergence must naturally await the evaluation of approximations for larger clusters.

A further point of interest is the validity of the scaling hypothesis, Eq. (3). The data collapse shown in Fig. 6, a plot of $\rho^* = \Delta_n^{-\beta}\rho_{a,n}$ versus $x = (\zeta - \zeta_{c,n})/\Delta_n$ provides support for the hypothesis. (In Ref. [30] a similar collapse is demonstrated for the Domany-Kinzel model.)

B. CAM analysis for $\nu_{||}$

As shown in Refs. [17–19], the CAM approach is readily extended to dynamics. Let

$$\gamma_n(\zeta) = -\frac{1}{\rho}\frac{d\rho}{dt} \tag{7}$$

be the relaxation rate in the n-site approximation, and let $\gamma(\zeta)$ be the true relaxation rate. Then we expect $\gamma \sim |\zeta - \zeta_c|^{\nu_{||}}$, while $\gamma_n \sim |\zeta - \zeta_{c,n}|^{\nu_{||,MF}}$ in the n-site approximation, where the mean-field exponent is $\nu_{||,MF} = 1$ for models with an absorbing-state phase transition [27]. A scaling hypothesis, analogous to Eq. (3), for the relaxation rate, is

$$\gamma_n(\zeta) = \Delta_n^{\nu_{||}} g\left(\frac{\zeta - \zeta_{c,n}}{\Delta_n}\right), \tag{8}$$

where the scaling function g vanishes when its argument is zero. Supposing that $g(x) \sim |x|^{\nu_{||,MF}}$, we see that $\gamma_n(\zeta) \sim \overline{\gamma}_n|\zeta - \zeta_{c,n}|$, where the amplitude follows

$$\overline{\gamma}_n \sim \Delta_n^{\nu_{||} - \nu_{||,MF}}. \tag{9}$$

I determine the relaxation rate numerically for $\zeta \lesssim \zeta_{c,n}$, and from these data extract the amplitudes $\overline{\gamma}_n$. The results, shown in Fig. 7, display substantial curvature on a log-log plot, so that direct determination of the critical exponent $\nu_{||}$ is not feasible. Simulations [16,26] yield estimates for $\nu_{||}$ in the range 2.3 - 2.6. The CAM results are consistent with values in this range, if we include a correction to scaling. The solid line in Fig. 7 is given by

$$\ln \overline{\gamma}_n = 1.5 \ln \Delta_n + A\Delta_n - B, \tag{10}$$

with fit parameters $A = 7.435$ and $B = 2.125$, consistent with a correction to scaling expression $\overline{\gamma}_n \propto \Delta_n^{\nu_{||}-1}(1 + A\Delta_n)$, with $\nu_{||} = 2.5$. While results for larger clusters will be needed to determine $\nu_{||}$ with precision, one can at least assert that the present results are consistent with the rather imprecise estimates from simulations.

VI. DISCUSSION

I have devised a computational algorithm for generating n-site cluster approximations for a one-dimensional stochastic sandpile model with a fixed particle density. To facilitate the analysis I impose the height restriction $z_i \leq 2$. Analyzing the results for $n \leq 11$, I obtain the estimates $\zeta_c = 0.930(1)$, $\beta = 0.41(1)$ and $\nu_{||} \simeq 2.5$, all in agreement with simulation [26]. While the results are not very precise, they provide significant independent support for the simulational findings, showing that FES models with a strict activity threshold belong to a universality class distinct from that of directed percolation (DP) [21–23]. Sandpile models in which sites with an above-threshold height can remain stable (so-called "sticky grains"), have recently been shown to belong to the DP class [32], but such is not the case for the model studied here. Application of the methods used in this work to other sandpile models should prove illuminating.

Acknowledgments

I thank Mário de Oliveira, Tânia Tomé, Attila Szolnoki, Gyorgy Szabó, Géza Ódor, and Paulo Alfredo Gonçalves Penido for helpful comments. This work was supported by CNPq, and CAPES, Brazil.

† e-mail: dickman@fisica.ufmg.br

REFERENCES

[1] P. Bak, C. Tang and K. Wiesenfeld, Phys. Rev. Lett. **59**, 381 (1987); Phys. Rev. A **38**, 364 (1988).

[2] D. Dhar, Physica A **263** (1999) 4, and references therein.

[3] R. Dickman, M. A. Muñoz, A. Vespignani, and S. Zapperi, Braz. J. Phys. **30**, 27 (2000). e-print: cond-mat/9910454.

[4] M. A. Muñoz, R. Dickman, R. Pastor-Satorras, A. Vespignani, and S. Zapperi, in *Modeling Complex Systems*, Proceedings of the 6th Granada Seminar on Computational J. Marro and P. L. Garrido, eds., AIP Conference Proceedings v. 574 (2001); e-print: cond-mat/0011442.

[5] R. Dickman, Physica A, in press; e-print: cond-mat/0110043.

[6] G. Grinstein, in *Scale Invariance, Interfaces and Nonequilibrium Dynamics*, *NATO Advanced Study Institute, Series B: Physics*, vol. 344, A. McKane et al., Eds. (Plenum, New York, 1995).

[7] C. Tang and P. Bak, Phys. Rev. Lett. **60**, 2347 (1988).

[8] A. Vespignani and S. Zapperi, Phys. Rev. Lett. **78**, 4793 (1997); Phys. Rev. E **57**, 6345 (1998).

[9] R. Dickman, A. Vespignani and S. Zapperi, Phys. Rev. E **57**, 5095 (1998).

[10] A. Vespignani, R. Dickman, M. A. Muñoz, and Stefano Zapperi, Phys. Rev. Lett. **81**, 5676 (1998).

[11] M. A. Muñoz, R. Dickman, A. Vespignani, and Stefano Zapperi, Phys. Rev. E **59**, 6175 (1999).

[12] A. Chessa, E. Marinari and A. Vespignani, Phys. Rev. Lett. **80**, 4217 (1998).

[13] A. Montakhab and J. M. Carlson, Phys. Rev. E **58**, 5608 (1998).

[14] V. B. Priezzhev, J. Stat. Phys. **74**, 955 (1994); E. V. Ivashkevich, J. Phys. A **27**, 3643 (1994); E. V. Ivashkevich,D.V.Ktitarev and V. B. Priezzhev, Physica A **209**, 347 (1994).

[15] A. Vespignani, R. Dickman, M. A. Muñoz, and S. Zapperi, Phys Rev. E**62**, 4564 (2000).

[16] R. Dickman, M. Alava, M. A. Muñoz, J. Peltola, A. Vespignani, and S. Zapperi, Phys Rev. E**64**, 056104 (2001).

[17] M. Suzuki and M. Katori, J. Phys. Soc. Jpn. **55**, 1 (1986).

[18] M. Suzuki, M. Katori, and X. Hu, J. Phys. Soc. Jpn. **56**, 3092 (1987).

[19] N. Konno and M. Katori, J. Phys. Soc. Jpn. **59**, 1581 (1990).

[20] A. L. C. Ferreira and S. K. Mendiratta, J. Phys. A**26**, L145 (1993).

[21] M. Rossi, R. Pastor-Satorras, and A. Vespignani, Phys. Rev. Lett. **85**, 1803 (2000).

[22] R. Pastor-Satorras and A. Vespignani, Phys. Rev. E**62**, 5875 (2000).

[23] S. Lübeck, Phys. Rev. E**64**, 016123 (2001); Eur. Phys. J. B**26**, 75 (2002).

[24] S. S. Manna, J. Phys. A **24**, L363 (1991).

[25] S. S. Manna, J. Stat. Phys. **59**, 509 (1990).

[26] R. Dickman, T. Tomé, and M. J. de Oliveira, e-print: cond-mat/0203565.

[27] J. Marro and R. Dickman *Nonequilibrium Phase Transitions in Lattice Models* (Cambridge University Press, Cambridge, 1999).

[28] W. H. Press, B. P. Flannery, S. A. Teukolsky, and W. T. Vetterling, *Numerical Recipes* (Cambridge University Press, Cambridge, 1996).

[29] M. E. Fisher, in *Proceedings of the International Summer School 'Enrico Fermi', Course*

LI, (Academic Press, New York, 1971); M. E. Fisher and M. N. Barber, Phys. Rev. Lett. **28**, 1516 (1972).
[30] T. Tomé and M. J. de Oliveira, Physica A**260**, 99 (1998).
[31] G. Grinstein, Z. W. Lai, and D. A. Browne, Phys. Rev. A **40**, 4820 (1989).
[32] P. K. Mohanty and D. Dhar, preprint: cond-mat/0202345.

TABLES

Transition	Probability
$020 \to 101$	1/2
$\to 200$	1/4
$120 \to 201$	1/2
$\to 102$	1/4
$\to 210$	1/4
$121 \to 202$	1/2
$\to 211$	1/4
$220 \to 202$	1/4
$\to 211$	1/2
$122 \to 212$	3/4

Transition probabilities for the restricted-height sandpile. Probabilitites are symmetric under reflection.

n	$\zeta_{c,n}$
1	0.5
2	0.75
3	0.80854
4	0.83682
5	0.85305
6	0.86378
7	0.87148
8	0.87736
9	0.88207
10	0.88594
11	0.88918

Table II. Critical densities in the n-site approximation.

FIGURE CAPTIONS

FIG. 1. Active-site density ρ versus $D = \max_{\mathcal{C}} \ |dP(\mathcal{C})/dt|$, for $n=10$, $\zeta=0.8860$.

FIG. 2. Stationary active-site density ρ versus particle density ζ. Solid curves: n-site approximations for n = 3 - 11; points: simulation results for a system of 5000 sites.

FIG. 3. Critical point shift $\Delta_n^{\nu_\perp}$ versus$1/n$. The solid line is a fit including a correction term as described in the text.

FIG. 4. $\rho'_n \equiv d\rho_{a,n}/d\zeta$ versus Δ_n. The derivative is evaluated at $x=1/4$. The slope of the solid line is -0.592, corresponding to $\beta = 0.408$.

FIG. 5. Active-site density $\rho_{a,n}(\zeta_c)$ versus δ_n. The slope of the solid line is 0.408.

FIG. 6. Scaled active-site density $\rho^* = \Delta_n^{-\beta}\rho_{a,n}$ versus scaled particle density $x = (\zeta - \zeta_{c,n})/\Delta_n$, for $n=6$ - 11.

FIG. 7. Relaxation rate amplitude $\overline{\gamma}_n$ versus Δ_n. The solid curve is a fit including a correction to scaling term as described in the text.

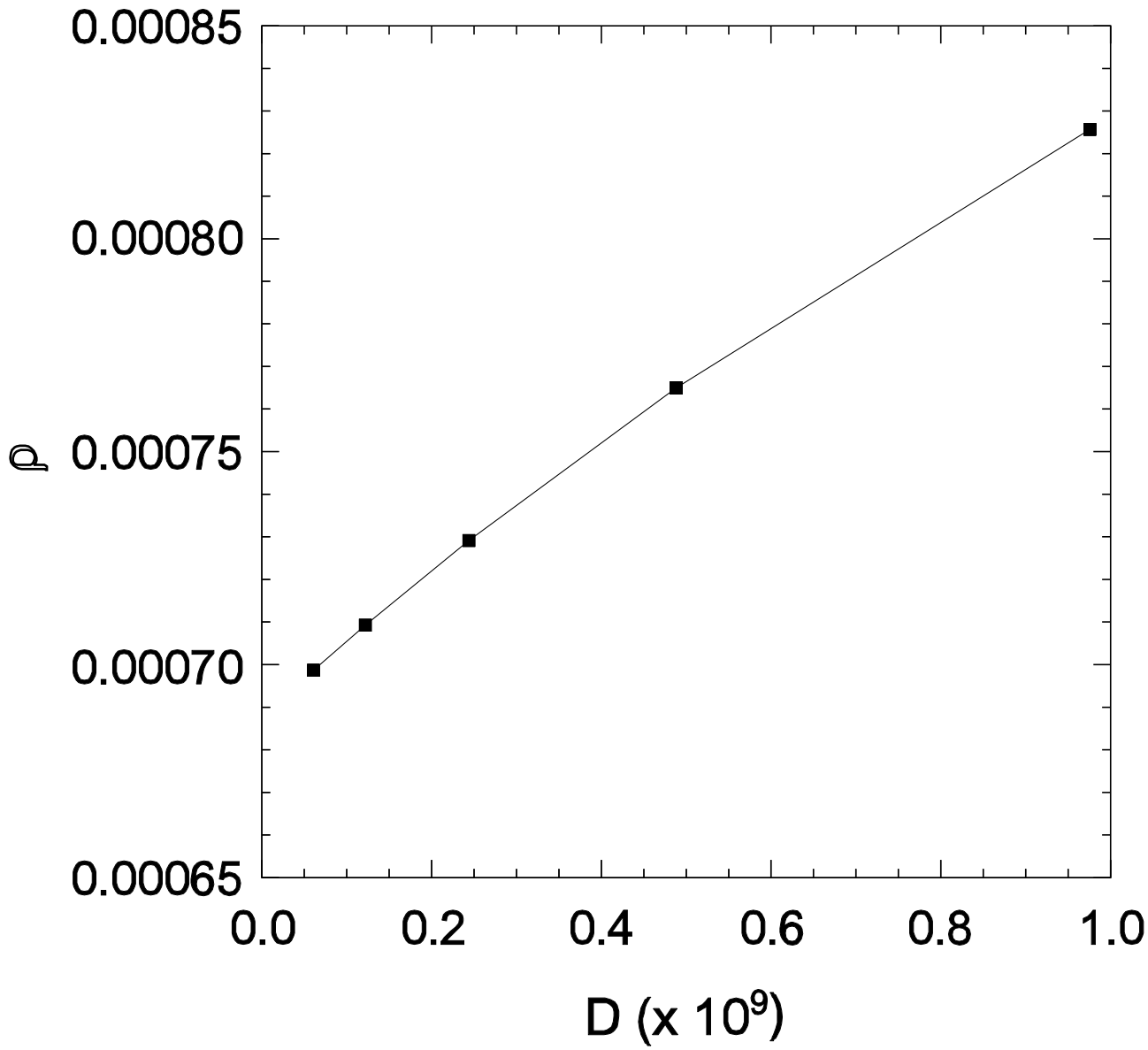
0.00085
0.00080
0.00075
0.00070
0.00065
a
0.0
0.2
0.4
0.6
0.8
1.0
D (x 10^9)

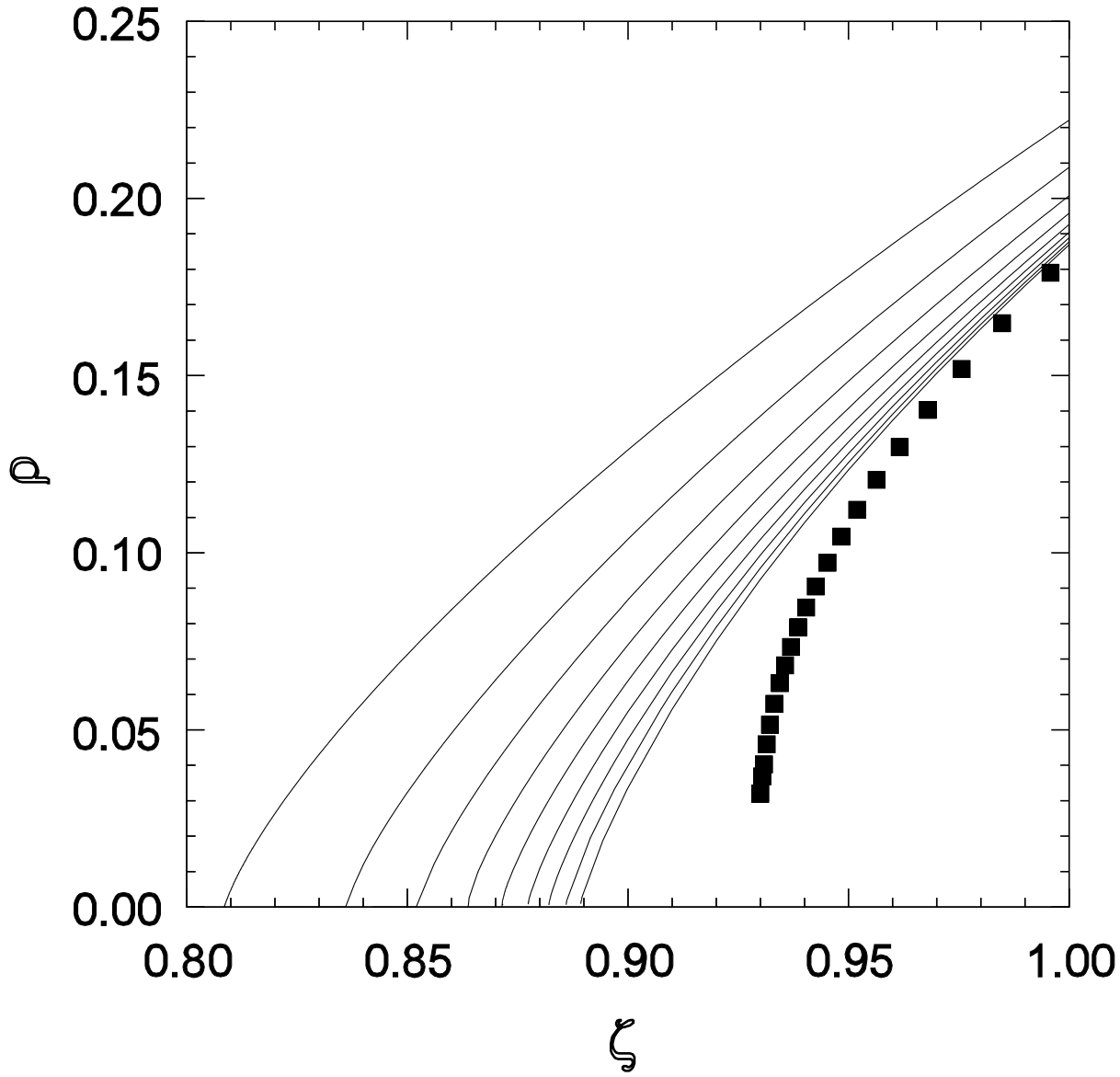
0.25
0.20
0.15
0.10
0.05
0.00
q
0.80
0.85
0.90
0.95
1.00
ζ

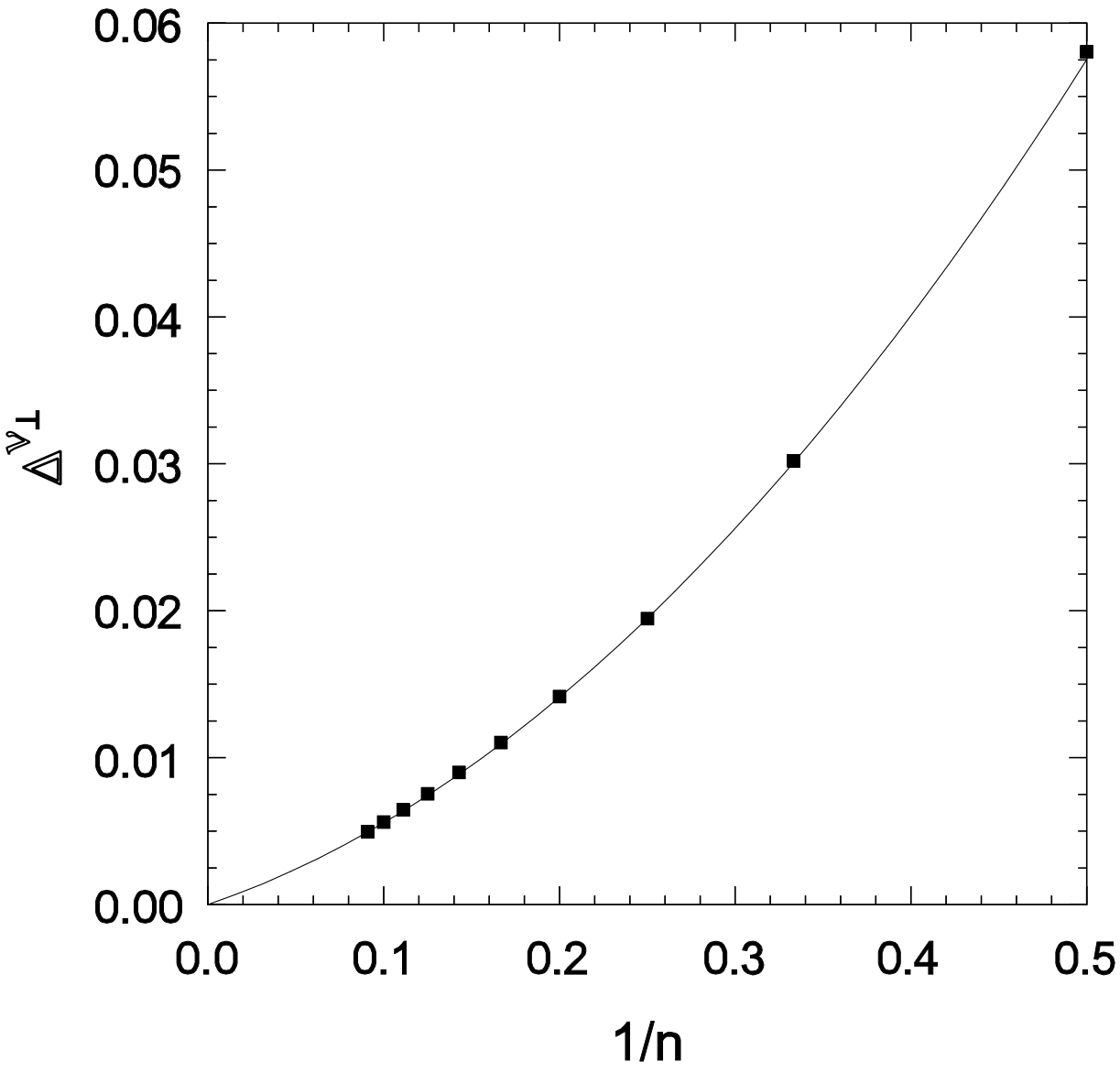
0.06
0.05
0.04
0.03
0.02
0.01
0.00
Δ^{ν}_{T}
0.0
0.1
0.2
0.3
0.4
0.5
1/n

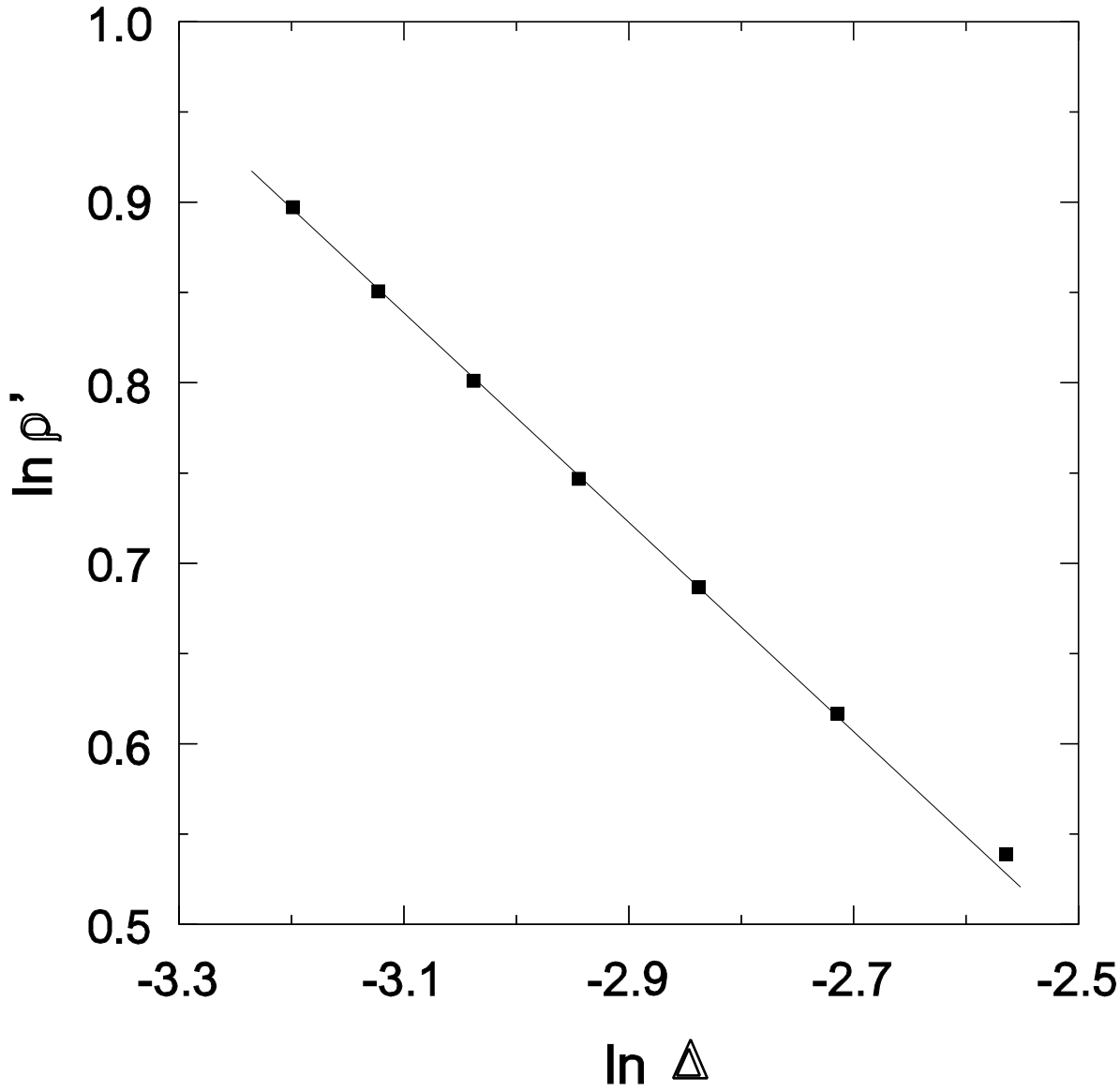
1.0
0.9
0.8
0.7
0.6
0.5
ln ρ'
-3.3
-3.1
-2.9
-2.7
-2.5
ln Δ

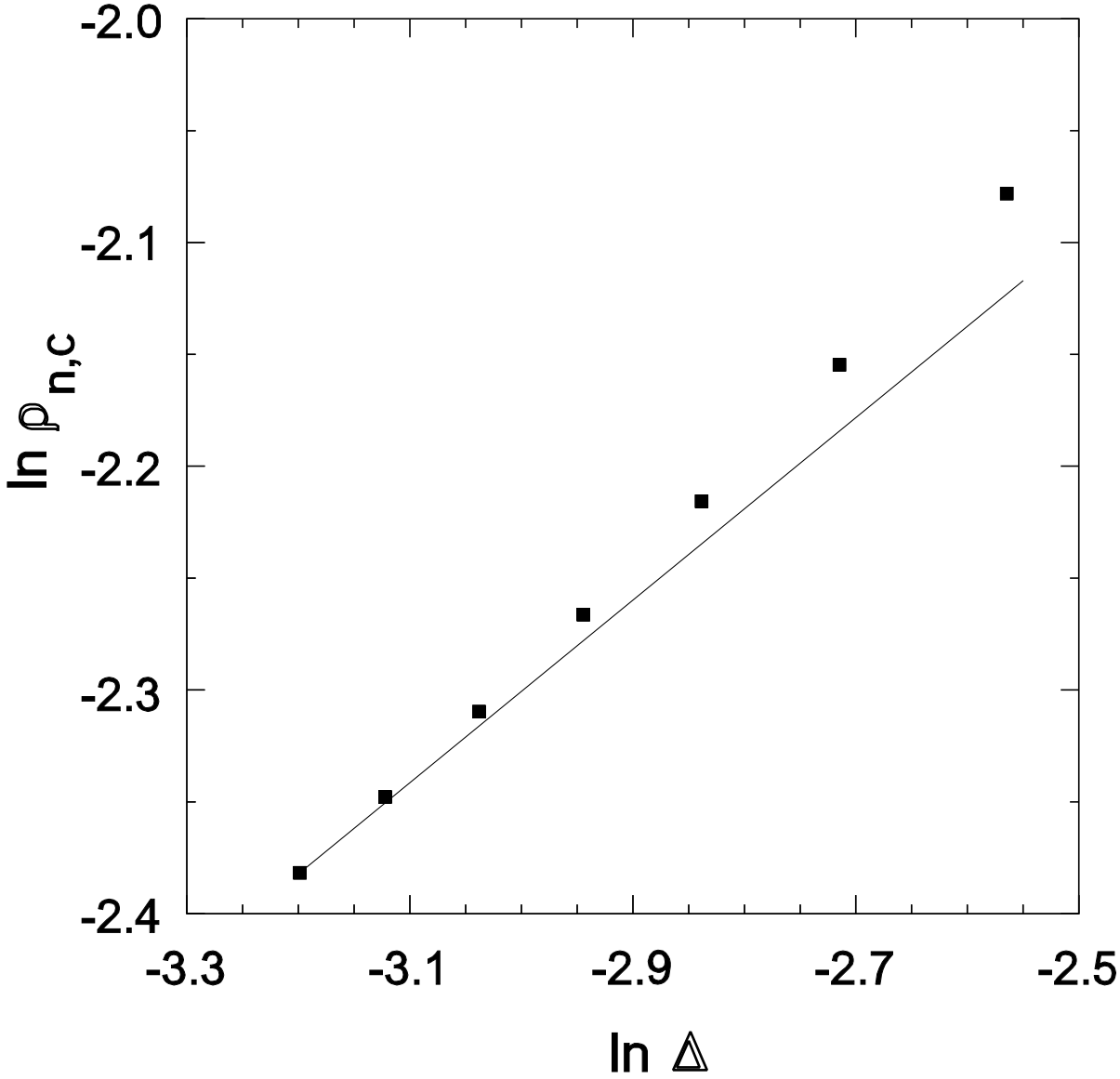
-2.0
-2.1
-2.2
-2.3
-2.4
ln ρn,c
-3.3
-3.1
-2.9
-2.7
-2.5
ln Δ

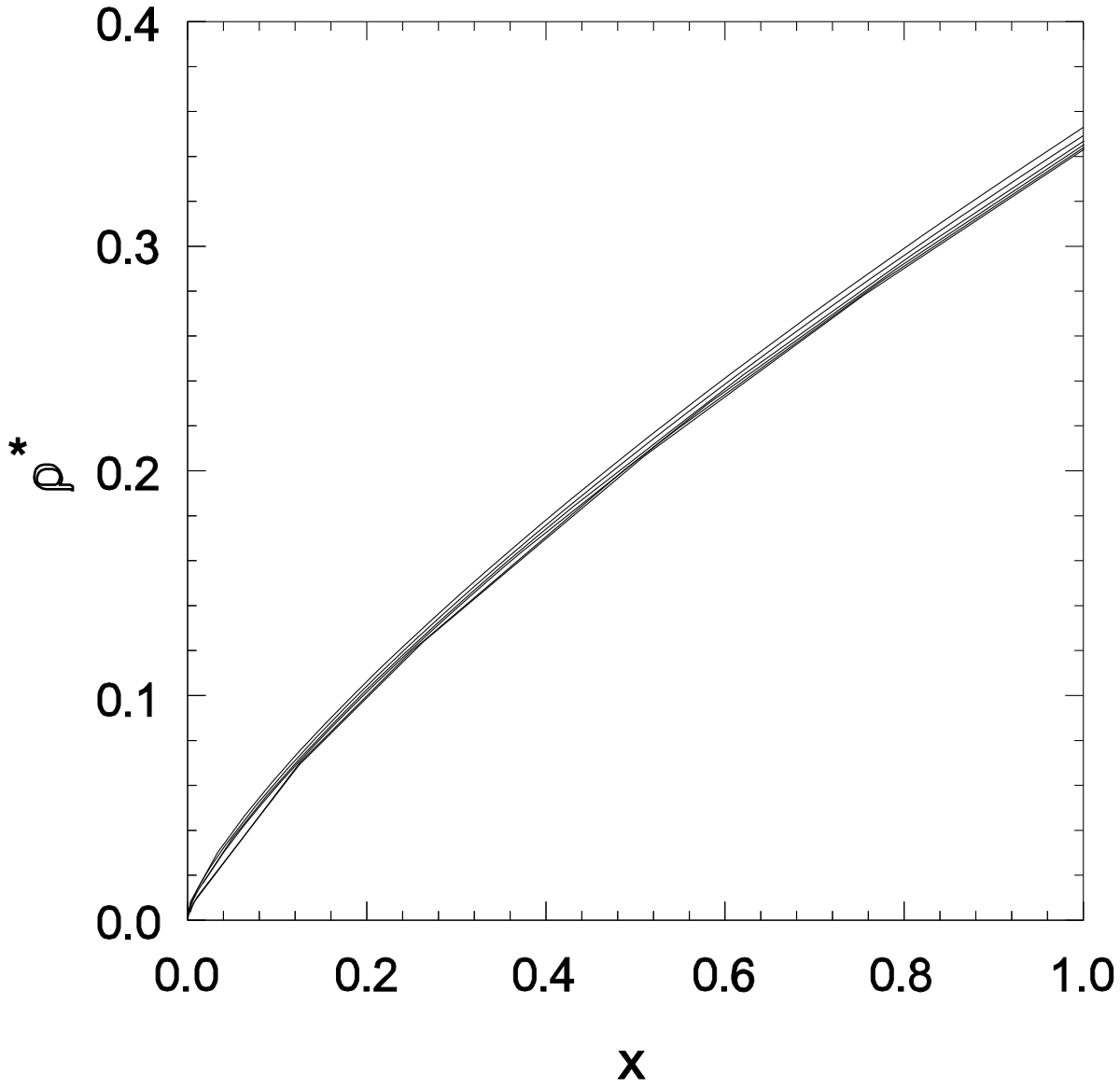
0.4
0.3
0.2
0.1
0.0
*
0.0
0.2
0.4
0.6
0.8
1.0
x

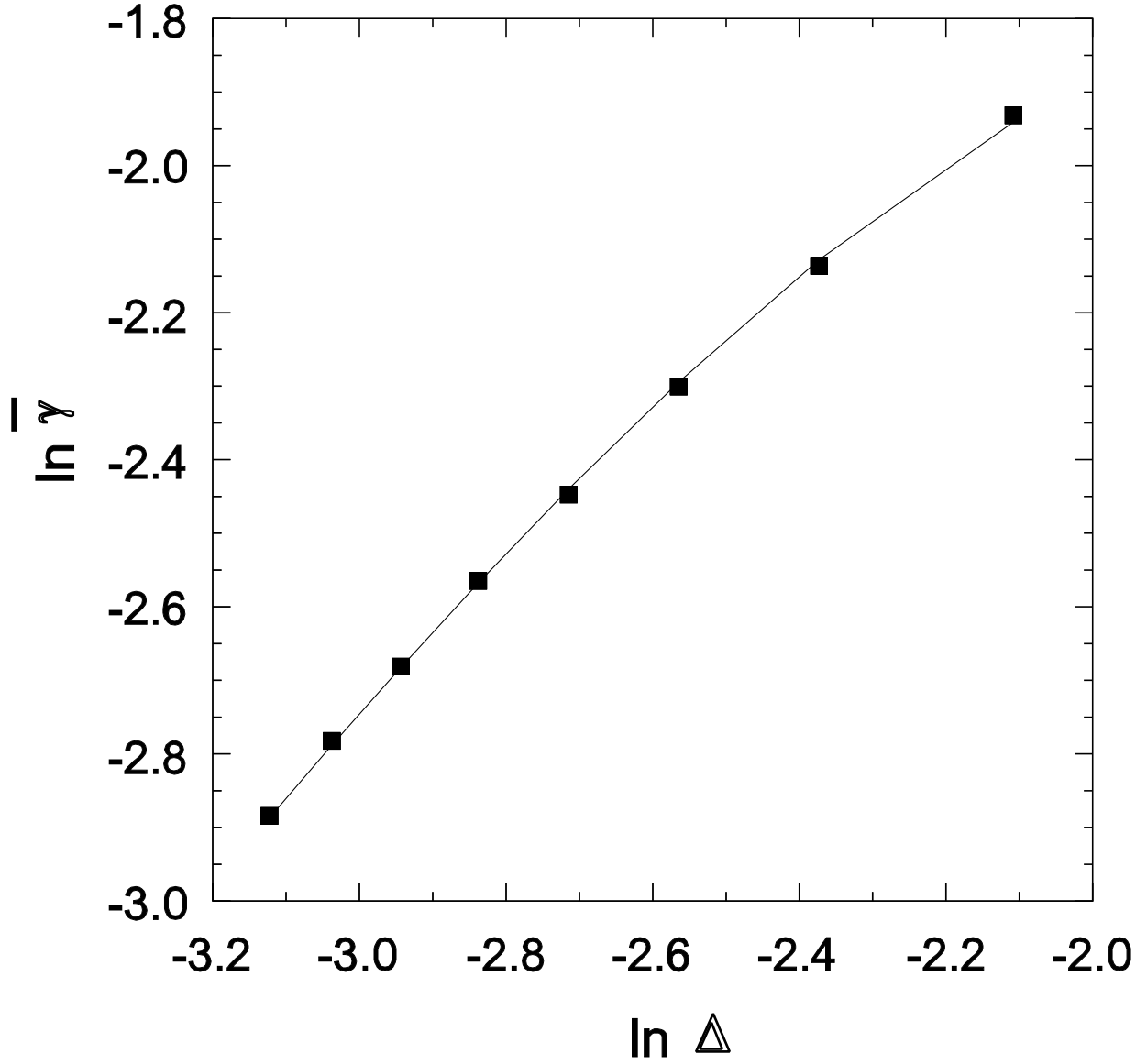
-1.8
-2.0
-2.2
-2.4
-2.6
-2.8
-3.0
ln γ
-3.2
-3.0
-2.8
-2.6
-2.4
-2.2
-2.0
ln Δ